Kobe University Repository : Kernel

PDF issue: 2025-12-05

A novel in vitro co-culture model to examine contact formation between astrocytic processes and cerebral vessels

Kawauchi, Shoji
Horibe, Sayo
Sasaki, Naoto
Hirata, Ken-ichi
Rikitake, Yoshiyuki

(Citation)
Experimental Cell Research,374(2):333-341

(Issue Date)
2019-01-15

(Resource Type)
journal article

(Version)
Accepted Manuscript

(Rights)
© 2018 Elsevier Inc.
This manuscript version is made available under the CC-BY-NC-ND 4.0 license
http://creativecommons.org/licenses/by-nc-nd/4.0/

(URL)
https://hdl.handle.net/20.500.14094/90007205

KOBE UNIVERSITY

A novel *in vitro co-culture* model to examine contact formation between astrocytic processes and cerebral vessels

Shoji Kawauchi[a], Sayo Horibe[b], Naoto Sasaki[b], Ken-ichi Hirata[c], Yoshiyuki Rikitake[b,*]

[a]Educational and Research Center for Clinical Pharmacy, Kobe Pharmaceutical University, Kobe 658-8558, Japan.

[b]Laboratory of Medical Pharmaceutics, Kobe Pharmaceutical University, Kobe 658-8558, Japan.

[c]Division of Cardiovascular Medicine, Department of Internal Medicine, Kobe University Graduate School of Medicine, Kobe 650-0017, Japan.

[*]**Correspondence to:** Yoshiyuki Rikitake, M.D., Ph.D. (ORCID: 0000-0001-7207-4656)
Laboratory of Medical Pharmaceutics, Kobe Pharmaceutical University, 4-19-1, Motoyamakitamachi, Higashinada-ku, Kobe 658-8558, Japan.
Tel.: +81-78-441-7578; Fax: +81-78-441-7578; E-mail: rikitake@kobepharma-u.ac.jp

Abstract

Here, we developed a novel *in vitro* co-culture model, in which process-bearing astrocytes and isolated cerebral microvessels from mice were co-cultured. Astrocytes formed contacts with microvessels from both adult and neonatal mice. However, concentrated localization of the immunofluorescence signal for aquaporin-4 (AQP4) at contact sites between perivascular endfoot processes and blood vessels was only detected with neonatal mouse microvessels. Contact between astrocytic processes and microvessels was retained, whereas concentrated localization of AQP4 signal at contact sites was lost, by knockdown of dystroglycan or α-syntrophin, reflecting polarized localization of AQP4 at perivascular regions in the brain. Further, using our *in vitro* co-culture model, we found that astrocytes predominantly extend processes to pericytes located at the abluminal surface of microvessels, providing additional evidence that this model is representative of the *in vivo* situation. Altogether, we have developed a novel *in vitro* co-culture model that can reproduce aspects of the *in vivo* situation and is useful for assessing contact formation between astrocytes and blood vessels.

Highlights

- A novel *in vitro* model was constructed by co-culturing process-bearing astrocytes and isolated cerebral microvessels from neonatal mice.
- The polarized localization of AQP4 was detected at contact sites between astrocyte processes and microvessels.
- The polarized localization of AQP4 at contact sites was disturbed by knockdown of α-syntrophin or dystroglycan.
- Astrocytes predominantly extended their processes to pericytes located at the abluminal surface of microvessels.

Keywords: α-syntrophin, aquaporin-4, dystroglycan, endfoot process, pericyte

Abbreviations: 2D, two-dimensional; 3D, three-dimensional; Ab, antibody; AQP4, aquaporin-4; BBB blood–brain barrier; BSA, bovine serum albumin; DAPI, 4',6-diamidino-2-phenylindole, dihydrochloride; DG, dystroglycan; DGC, dystrophin–glycoprotein complex; DIV, days *in vitro*; E, embryonic day; FAK, focal adhesion kinase; GFAP, glial fibrillary acidic protein; mAb, monoclonal Ab; NVU, neurovascular unit; PDGFR, platelet-derived growth factor receptor; P, postnatal day; pAb, polyclonal Ab; qPCR, quantitative real-time reverse transcriptase polymerase chain reaction; RRIDs, Research Resource Identifier; si, small interfering

Introduction

Brain blood vessels (endothelial cells, pericytes, smooth muscle cells, and basal lamina) and neuronal cells (neurons, astrocytes, microglia, and oligodendrocytes) form a structurally and functionally integrated unit called the neurovascular unit (NVU) [1]. Each NVU component closely communicates with the others. The NVU functions to couple neuronal activity to vascular function, thereby maintaining brain homeostasis and the microenvironment. As the importance of the NVU in maintaining brain homeostasis and the microenvironment has gradually become clear, it is recognized that communication between the NVU components is extremely complex. Nonetheless, in-depth understanding of this communication is crucial for investigating neurovascular and neurodegenerative diseases such as stroke and Alzheimer's disease. Essential tools in this regard include experimental NVU models. *In vitro* NVU models are useful for understanding the different roles and functions of cells comprising the NVU, as well as assessing the effect of therapeutic compounds on neural function after crossing the endothelial barrier [2]. Moreover, these models have the potential to reduce animal use [3]. *In vitro* NVU models can roughly be classified into two categories: two-dimensional (2D) and three-dimensional (3D) models. The 2D co-culture model has been widely used for blood–brain barrier (BBB) research [4, 5]. For example, brain endothelial cells can be seeded onto culture inserts and astrocytes grown on the underside of the inserts. Otherwise, instead of astrocytes, pericytes can be co-cultured on the underside of the insert and astrocytes grown on the bottom of the well in which the insert sits. Alternatively, in contrast to 2D models, various 3D co-culture models of endothelial cells, pericytes, and astrocytes have recently been developed to specifically mimic the *in vivo* microenvironment [6-8]. Altogether, these *in vitro* models are useful for studying NVU roles in various diseases as well as drug screening. However, for correct interpretation of the obtained results, the strengths and weaknesses of each model must be understood and used appropriately in accordance with the respective research purpose.

In the NVU, astrocytes are uniquely located between blood vessels and neurons. They extend processes to the basement membrane of blood vessels (called perivascular endfoot processes), which enwrap blood vessels, and to synapses (called perisynaptic process ensheathing synapses). Astrocytes can thereby regulate the BBB [9] and regional cerebral blood flow [10], and ultimately provide structural, trophic, and metabolic support to neurons. The water channel aquaporin-4 (AQP4) [11] is localized in a concentrated manner at contact sites formed between perivascular endfoot processes and blood vessels. Moreover, dystrophin–glycoprotein complex (DGC) proteins, which are comprised of Dp71, dystroglycan (DG), α-dystrobrevin, and α-syntrophin, are critical for polarized localization of AQP4 at perivascular regions of the brain [12-14]. DG is cleaved into two proteins: extracellular α-DG, which binds to laminin, a major component of the basement membrane of blood

vessels, and transmembrane β-DG, which intracellularly binds to dystrophin and subsequently links to α-syntrophin and anchors AQP4.

Astrocytes are often used in various *in vitro* NVU models. In culture, astrocytes exhibit a flat, epithelioid morphology with no or very few processes, which is quite different from the star-shaped, process-bearing morphology *in vivo*. To overcome this morphological problem, we established a novel method for obtaining process-bearing astrocytes by differentiation of neurospheres [15]. These process-bearing astrocytes enabled us to investigate the mechanism of process formation and branching of astrocytes. For example, using these astrocytes, we found a key role for the interaction between laminin and DG in process formation and branching [16]. In the present study, we used these astrocytes to develop a novel *in vitro* co-culture model by which we can assess contact formation between astrocytes and blood vessels.

Materials and Methods

Antibodies

Isolectin B4-Alexa Fluor® 488 conjugate and rat anti- glial fibrillary acidic protein (GFAP) monoclonal antibody (mAb) were purchased from Thermo Fisher Scientific (Waltham, MA, USA; #13-0300, RRID:AB_2532994). Rabbit anti-AQP4 polyclonal antibody (pAb) was purchased from Sigma–Aldrich (St. Louis, MO, USA; #HPA014784, RRID:AB_1844967). Rabbit anti- Platelet-derived growth factor receptor (PDGFR)-β mAb was purchased from Abcam (Cambridge, UK ; #ab32570, RRID:AB_777165). Primary Abs were visualized using goat fluorochrome-conjugated AlexaFluor 405 (Thermo Fisher Scientific; #A-31556, RRID:AB_221605) and 568 (Thermo Fisher Scientific; #A-11077, RRID:AB_2534121) secondary Abs.

Preparation of Astrocytes

Mouse astrocyte cultures were prepared by differentiation of neural stem/progenitor cells in neurospheres prepared from C57BL/6 mouse pups, as described previously [16]. In brief, neurospheres were generated from mouse pups at P1 (n = 7) according to the protocol by Chojnacki and Weiss [17]. Generated neurospheres were dissociated by treatment of 0.25% trypsin–EDTA solution (Nacalai Tesque Inc., Kyoto, Japan), and cultured in Dulbecco's modified Eagle's medium/F-12 (Wako Pure Chemical Corporation, Osaka, Japan; #042-30555) containing 1% N2 supplement (Wako Pure Chemical Corporation; #141-08941), 5×10^3 units/ml leukemia inhibitory factor (Wako Pure Chemical Corporation; #199-16651), and 50 ng/ml bone morphogenetic protein-2 (R&D Systems, Minneapolis, MN, USA; #355-BEC/CF) for differentiation into astrocytes [17]. The protocol was approved by the

Animal Care Committee of Kobe Pharmaceutical University (Permit Numbers: 2015-039, 2016-018, 2017-027, 2018-004).

Isolation of Cerebral Microvessels from Mice

Cerebral microvessels were isolated from adult (13-week-old, male, *n* = 11) and neonatal (P1, *n* = 54) C57BL/6 mice (Japan SLC, Hamamatsu, Japan; RRID:IMSR_JAX:000664) according to the protocol by Boulay, *et al*. [18] with slight modifications. In brief, mouse brain was homogenized using a glass potter homogenizer (20 strokes) in B1 solution (1.5 ml of 1M HEPES [Nacalai Tesque Inc.] to 150 ml Hanks' Balanced Salt Solution [Nacalai]). The homogenate was centrifuged at 2,000 × *g* for 10 min at 4°C, and the pellet suspended in a buffer with 1.8 g of dextran (Sigma–Aldrich; #31390) added to 10 ml B1 solution. The suspending solution was centrifuged at 4,400 × *g* for 15 min at 4°C, and the pellet suspended in B1 solution containing 1% bovine serum albumin (BSA) (Wako Pure Chemical Corporation). Cerebral microvessels were isolated by filtering the suspended solution through a 20, 40, or 100 μm mesh filter.

Co-culture of Astrocytes with Isolated Cerebral Microvessels

Dissociated neurospheres (1.4–3.0 $\times$ 10^4 cell/ml) were co-cultured with isolated cerebral microvessels (100 μl/well) on coverslips pre-coated with poly-L-ornithine (Wako Pure Chemical Corporation; #16327421) and mouse Engelbreth–Holm–Swarm laminin (Corning Inc., Corning, NY, USA; #354232). Neurospheres were cultured in Dulbecco's modified Eagle's medium/F-12 containing 1% N2 supplement, 10^9 units/ml leukemia inhibitory factor, and 50 ng/ml bone morphogenetic protein-2 for differentiation into astrocytes.

Immunofluorescence Microscopy

Immunofluorescence microscopy was essentially performed as described previously [19]. For co-culture staining, astrocytes with isolated cerebral microvessels were fixed using 2% paraformaldehyde for 20 min, and then blocked with Blocking One Histo (Nacalai Tesque Inc.) at room temperature for 10 min, before washing using phosphate-buffered saline containing Tween 20. For cerebral section staining, adult (13-week-old, male, *n* = 3) and neonatal (P1, *n* = 3) C57BL/6 mice (Japan SLC) were deeply anesthetized by isoflurane inhalation. Whole brains were fixed with 10% paraformaldehyde at room temperature overnight. They were then soaked in 20% sucrose for 2 hours at room temperature and finally overnight at 4°C in 25% sucrose. Whole brains were embedded in OCT compound (Sakura Finetek, Torrance, CA, USA). Cryostat sections were incubated with 1% BSA, 10% normal goat serum, and 0.5% Triton X-100 in phosphate-buffered saline at room temperature for 60 min. Samples were

stained with the indicated Abs (cultured astrocytes, 1:200; cerebral section, 1:300), followed by appropriate fluorophore-conjugated secondary Abs (cultured astrocyte, 1:200; cerebral section, 1:300). Confocal image analysis was performed on a confocal laser-scanning microscope (LSM700; Carl Zeiss, Oberkochen, Germany) using a 20× objective lenses (Plan Apochromat with a numerical aperture of 0.8 DICIII; Carl Zeiss). Images captured on the LSM 700 at room temperature were analyzed using ZEN acquisition software (Carl Zeiss).

Transfection of Small Interfering RNAs

Dissociated neurospheres were transfected with Stealth RNAis for DG and α-syntrophin, or a non-silencing negative control (Invitrogen, Carlsbad, CA, USA) using Lipofectamine RNAiMAX (Invitrogen), according to the manufacturer's instructions. Neurospheres were then plated onto coverslips and co-cultured with isolated cerebral microvessels. We previously reported markedly reduced mRNA expression of DG and α-syntrophin in astrocytes transfected with these siRNAs [16].

Time-lapse Imaging

Dissociated neurospheres were co-cultured with isolated cerebral microvessels for 5 hours, as described above. Time-lapse images of contact formation between extending astrocytic processes and microvessels were then captured every 15 minutes on a BZ-800 microscope (Keyence, Tokyo, Japan) with 5% O_2 and 95% air at 37°C for the successive 20 hours. A movie was generated from the images at a rate of 3 frames/sec. After capturing the images, samples were subjected to immunofluorescence microscopy.

Statistical Analysis

All experiments were performed at least three times. Contact formation between astrocytic processes and microvessels were analyzed by Pearson's chi-square test (SPSS v22.0; IBM Corporation, Armonk, NY, USA).

Results

Contact Formation Between Astrocytic Processes and Cerebral Microvessels Isolated from Adult Mice

We recently established a novel method for obtaining cultured astrocytes with a rich complexity of processes [16]. Here, using these astrocytes, we sought to develop a novel co-culture model that would be applicable for *in vitro* assessment of contact formation between astrocytes and cerebral microvessels. Neurospheres were dissociated (**Fig. 1A, arrow**) and co-cultured for 4 days *in vitro*

(DIV), with cerebral microvessels isolated from mice at 13 weeks of age. Dissociated cells were differentiated into astrocytes with extended processes, which appeared to contact microvessels (**Fig. 1A, arrowheads**). These differentiated astrocytes were immunopositive for anti-GFAP (**Fig. 1B**). Immunofluorescence signal for AQP4 was observed, but because of residual strong signal for AQP4 in the isolated microvessels, it was unclear whether this AQP4 signal was concentrated at contact sites formed between astrocytic processes and microvessels (**Fig. 1B, arrowheads**). Thus, we have developed a novel co-culture system for astrocytes and microvessels, with contact shown between astrocytic processes and microvessels. However, at this stage, it was still unclear whether AQP4 is concentrated at these contact sites.

Absence of GFAP and AQP4 Expression Around Cerebral Microvessels in Neonatal Mice

We next sought to isolate microvessels from neonatal mice. Cerebral sections were prepared from adult and neonatal mice and subjected to immunofluorescence staining with isolectin B4, anti-GFAP mAb, and anti-AQP4 pAb (**Fig. 2A**). In adult mice, immunofluorescence signal for AQP4 was observed around microvessels (**Fig. 2A, arrowheads**) and along the glia limitans at the pial surface of the cerebral cortex (**Fig. 2A, arrow**). In contrast, in neonatal mice, immunofluorescence signal for AQP4 was observed along the glia limitans at the pial surface of the cerebral cortex (**Fig. 2A, arrow**), but not around microvessels (**Fig. 2A, arrowheads**). In addition, immunofluorescence signal for GFAP was observed along the glia limitans (**Fig. 2A, arrow**) but not around microvessels (**Fig. 2A, arrowheads**). These results suggest that astrocytes are not yet (or only a few) present in the parenchyma of the cerebral cortex of neonatal mice. Thus, no AQP4 signal was observed in this region.

We then isolated microvessels from the cerebral cortex of neonatal mice and stained them using isolectin B4, anti-GFAP mAb, and anti-AQP4 pAb (**Fig. 2B**). In contrast to the positive staining in microvessels isolated from adult mice, immunofluorescence signals for GFAP and AQP4 were not observed in microvessels isolated from neonatal mice, which is in good agreement with our staining of cerebral sections.

Contact Formation Between Astrocytic Processes and Cerebral Microvessels Isolated from Neonatal Mice

Dissociated neurosphere cell suspensions (**Fig. 3A, arrow**) were co-cultured with microvessels isolated from neonatal mice. At 4 DIV, differentiated astrocytes appeared to contact microvessels (**Fig. 3A, arrowheads**). Immunofluorescence signal for GFAP was observed in differentiated astrocytes, but not isolated microvessels (**Fig. 3B**). Immunofluorescence signal for AQP4 was observed at contact sites between astrocytic processes and microvessels (**Fig. 3B, arrowhead**). These results suggest that co-

culture of astrocytes and isolated microvessels from neonatal mice can be used to examine contact formation between astrocytes and blood vessels, and consequently for further analyses.

To further examine contact formation between astrocytic processes and cerebral microvessels isolated from neonatal mice, we used orthogonal projections of confocal Z-stacks. Strong immunofluorescence signals were detected for GFAP and AQP4, which were closely located at contact sites between astrocytic processes and microvessels (**Fig. 3C**). Peaks in intensity profile for the immunofluorescence signal of AQP4 were observed, which were consistent with intensity profile peaks for GFAP, and adjacent to those for isolectin B4, indicating very close localization of the astrocytic process and microvessel (**Fig. 3D, [b] in left panel, [a] in right panel**). Overall, these results indicate successful *in vitro* reconstruction of contact sites between astrocytic processes and microvessels.

Effect of Knockdown of α-Syntrophin and DG on Concentration of Immunofluorescence Signal for AQP4 at Contact Sites Between Astrocytic Processes and Cerebral Microvessels Isolated from Neonatal Mice

To further determine whether our *in vitro* model successfully reproduces the *in vivo* situation, we examined the effect of α-syntrophin and DG knockdown on AQP4 localization. Following α-syntrophin or DG knockdown, astrocytes still contacted microvessels (**Fig. 4A, arrowheads**). Analysis of orthogonal projections of confocal Z-stacks demonstrated strong immunofluorescence signals for GFAP and AQP4, which were closely located at contact sites between astrocytic processes and microvessels (**Fig. 4A**). In control small interfering (si)RNA-transfected astrocytes, intensity profile peaks for the immunofluorescence signal of AQP4 were observed, which were consistent with intensity profile peaks for GFAP, and adjacent to those for isolectin B4 (**Fig. 4B, [d] in left panel, [a] in right panel**). However, in α-syntrophin and DG knockdown astrocytes, strong immunofluorescence signal for AQP4 was not observed adjacent to intensity profile peaks for isolectin B4 immunofluorescence signal. Meanwhile, the levels of AQP4 immunofluorescence signal were equivalent to levels for the other intensity profile peaks for AQP4 immunofluorescence signal (**Fig. 4C, [a] in left panel, [a] in right panel; Fig. 4D, [d] in left panel, [a] in right panel**). These results indicate that polarized localization of AQP4 is disturbed by knockdown of α-syntrophin or DG, and provide additional supporting evidence for successful reconstruction of our *in vitro* model.

Predominant Contact Formation of Astrocytic Processes to Pericytes Located at the Abluminal Surface of Microvessels

A recent study demonstrated that AQP4 predominantly localizes at contact sites between astrocytic endfoot processes and pericytes located at the abluminal surface of microvessels compared with

pericyte-uncovered regions [20, 21]. Therefore, we next examined the relationship between astrocytic processes and pericytes. PDGFRβ was used as a marker of perivascular pericytes. Immunofluorescence signal for GFAP was closely localized to PDGFRβ, suggesting that astrocytic processes contact pericytes at 1 and 3 DIV (**Fig. 5A**). Time-lapse imaging demonstrated that at 1 DIV, astrocytic processes appeared to extend randomly, but preferentially attached to pericytes (**Fig. 5B and Movie 1**). Quantitative analysis demonstrated that astrocytic processes formed contacts, almost twice as frequently, with vascular regions adjacent to PDGFRβ-positive pericytes compared with PDGFRβ-negative pericyte-uncovered regions both at 1 and 3 DIV (**Table 1**). There is no significant difference in frequency of contacts between 1 and 3 DIV (Pearson's chi-square test). Altogether, these results indicate that astrocytes predominantly extend their processes to pericytes located at the abluminal surface of microvessels.

Discussion

Here, we have developed a novel *in vitro* model by co-culture of astrocytes and cerebral microvessels isolated from mice. We recently developed a culture method for generating astrocytes exhibiting a rich complexity of processes, which we used here. In terms of microvessels, those isolated from neonatal mice were more beneficial than those from adult mice, because almost no immunofluorescence signal for AQP4 was observed in neonatal mouse microvessels. Pericytes are recruited to newly formed microvessels at embryonic day (E) 15.5 to E18.5 in mice [22]. At postnatal day (P) 4, microvessels are in direct contact with pericytes, but not astrocytes [23]. Therefore, our finding is consistent with these previous studies.

DGC proteins comprised of Dp71, DG, α-dystrobrevin, and α-syntrophin are critical for perivascular localization of AQP4 in the brain. Loss of DG or α-syntrophin in astrocytes results in loss of polarized localization of AQP4 [12, 14]. Consistent with this *in vivo* situation, we show here that polarized localization of AQP4 is disrupted by knockdown of DG or α-syntrophin in astrocytes. DG is a receptor for the extracellular matrix proteins, laminin and agrin. Delocalization of AQP4 is observed in laminin α2 knockout mice [24], but not agrin knockout mice [25], suggesting a critical role of laminin in polarized localization of AQP4. In the brain, laminin is particularly rich in the basement membrane. Laminins are formed by coiled-coil interactions of α, β, and γ chains. To date, there are five α, three β, and three γ chains described, giving rise to at least 18 isoforms [26]. Laminin-111 and -211 are astrocytic, while laminin-411 and -511 are endothelial and found in the basement membrane of brain microvessels [27]. Previous studies have shown that a lack of laminin causes several astrocytic

abnormalities [24, 28]. Collectively, interaction of DG in astrocytes with laminin in microvessels plays a pivotal role in perivascular localization of AQP4, and our model can reproduce this *in vivo* situation.

In the brain, compared with other perivascular regions, AQP4 is enriched at contact sites between astrocytic processes and pericytes [20, 21]. This implies that pericytes may guide polarized localization of AQP4. As described above, polarized localization of AQP4 is dependent on the interaction between astrocytic DG and laminin. This led us to hypothesize that laminin is predominantly localized at the basement membrane adjacent to pericytes. Indeed, astrocyte-derived parenchymal basement membrane shows defective deposition in pericyte-deficient NVU [20]. This suggests that astrocytic laminin-111 and -211 play critical roles in polarized localization of AQP4, which is further supported by delocalization of AQP4 in laminin α2 knockout mice [24]. More importantly, we also show that astrocytes predominantly extend their processes to pericytes located at the abluminal surface of microvessels, indicating that pericytes may guide process extension to blood vessels. However, if so, it remains unclear how pericytes guide process extension. Factors released by pericytes that guide process extension have yet to be identified, and our model may be of use in this regard.

Understanding development and maintenance of contact formation is fundamentally important not only to physiology but also to diseases in which communication between astrocytes and blood vessels may be disturbed [29]. However, considerable time and money is needed to screen the effects of certain drugs and clarify the roles of certain molecules using animal models of human disease. In our model, use of astrocytes and/or microvessels obtained from such animal models enables screening with less time, money, and effort. Of course, our model must be appropriately used in accordance with the respective research purpose and correct interpretation of the obtained results.

There are a couple of limitations to our model. First, the microvessels have no blood flow. Lack of blood flow may affect synthesis and/or release of chemoattractants from vascular endothelial cells and pericytes, which guide astrocytic processes to microvessels. Second, neuronal cells such as neurons, microglia, and oligodendrocytes are not included. Particularly, in addition to microvessels, astrocytes extend processes to neuronal synapses and in turn regulate synaptic transmission and plasticity. Physical and functional interaction between astrocytes and neurons may influence their interaction with microvessels. In addition, our model is 2D and not 3D. Thus, our *in vitro* model does not recapitulate all aspects of NVU complexity *in vivo*.

In conclusion, we developed a novel *in vitro* neurovascular unit model, and using this model found that astrocytes predominantly extend processes to pericytes located at the abluminal surface of microvessels. Thus, this model can reproduce aspects of the in vivo situation and is useful for assessing contact formation between astrocytes and blood vessels.

Acknowledgements

We thank Rachel James, Ph.D., from Edanz Group (www.edanzediting.com/ac) for editing a draft of this manuscript.**Competing Interests**

No competing interests declared.

Funding

This work was supported by the Japan Society for the Promotion of Science (JSPS) KAKENHI [16K08258 to Y.R.].

References

[1] E.H. Lo, T. Dalkara, M.A. Moskowitz, Mechanisms, challenges and opportunities in stroke, Nat Rev Neurosci 4 (2003) 399-415.

[2] G. Adriani, D. Ma, A. Pavesi, R.D. Kamm, E.L. Goh, A 3D neurovascular microfluidic model consisting of neurons, astrocytes and cerebral endothelial cells as a blood-brain barrier, Lab Chip 17 (2017) 448-459.

[3] M.E. Boutin, L.L. Kramer, L.L. Livi, T. Brown, C. Moore, D. Hoffman-Kim, A three-dimensional neural spheroid model for capillary-like network formation, J Neurosci Methods 299 (2018) 55-63.

[4] Y. He, Y. Yao, S.E. Tsirka, Y. Cao, Cell-culture models of the blood-brain barrier, Stroke 45 (2014) 2514-2526.

[5] H.C. Helms, N.J. Abbott, M. Burek, R. Cecchelli, P.O. Couraud, M.A. Deli, C. Forster, H.J. Galla, I.A. Romero, E.V. Shusta, M.J. Stebbins, E. Vandenhaute, B. Weksler, B. Brodin, In vitro models of the blood-brain barrier: An overview of commonly used brain endothelial cell culture models and guidelines for their use, J Cereb Blood Flow Metab 36 (2016) 862-890.

[6] A. Tourovskaia, M. Fauver, G. Kramer, S. Simonson, T. Neumann, Tissue-engineered microenvironment systems for modeling human vasculature, Exp Biol Med (Maywood) 239 (2014) 1264-1271.

[7] B.T. Hawkins, S. Grego, K.L. Sellgren, Three-dimensional culture conditions differentially affect astrocyte modulation of brain endothelial barrier function in response to transforming growth factor beta1, Brain Res 1608 (2015) 167-176.

[8] A. Herland, A.D. van der Meer, E.A. FitzGerald, T.E. Park, J.J. Sleeboom, D.E. Ingber, Distinct Contributions of Astrocytes and Pericytes to Neuroinflammation Identified in a 3D Human Blood-Brain Barrier on a Chip, PLoS One 11 (2016) e0150360.

[9] J.I. Alvarez, T. Katayama, A. Prat, Glial influence on the blood brain barrier, Glia 61 (2013) 1939-1958.

[10] G.C. Petzold, V.N. Murthy, Role of astrocytes in neurovascular coupling, Neuron 71 (2011) 782-797.

[11] S. Nielsen, E.A. Nagelhus, M. Amiry-Moghaddam, C. Bourque, P. Agre, O.P. Ottersen, Specialized membrane domains for water transport in glial cells: high-resolution immunogold cytochemistry of aquaporin-4 in rat brain, J Neurosci 17 (1997) 171-180.

[12] J.D. Neely, M. Amiry-Moghaddam, O.P. Ottersen, S.C. Froehner, P. Agre, M.E. Adams, Syntrophin-dependent expression and localization of Aquaporin-4 water channel protein, Proc Natl Acad Sci U S A 98 (2001) 14108-14113.

[13] G.P. Nicchia, A. Rossi, U. Nudel, M. Svelto, A. Frigeri, Dystrophin-dependent and -independent AQP4 pools are expressed in the mouse brain, Glia 56 (2008) 869-876.

[14] S. Noell, K. Wolburg-Buchholz, A.F. Mack, A.M. Beedle, J.S. Satz, K.P. Campbell, H. Wolburg, P. Fallier-Becker, Evidence for a role of dystroglycan regulating the membrane architecture of astroglial endfeet, Eur J Neurosci 33 (2011) 2179-2186.

[15] B.A. Reynolds, S. Weiss, Generation of neurons and astrocytes from isolated cells of the adult mammalian central nervous system, Science 255 (1992) 1707-1710.

[16] J. Sato, S. Horibe, S. Kawauchi, N. Sasaki, K.I. Hirata, Y. Rikitake, Involvement of aquaporin-4 in laminin-enhanced process formation of mouse astrocytes in 2D culture: Roles of dystroglycan and alpha-syntrophin in aquaporin-4 expression, J Neurochem (2018 preprint) [Epub ahead of print].

[17] A. Chojnacki, S. Weiss, Production of neurons, astrocytes and oligodendrocytes from mammalian CNS stem cells, Nat Protoc 3 (2008) 935-940.

[18] A.C. Boulay, B. Saubamea, X. Decleves, M. Cohen-Salmon, Purification of Mouse Brain Vessels, J Vis Exp (2015) e53208.

[19] H. Tawa, Y. Rikitake, M. Takahashi, H. Amano, M. Miyata, S. Satomi-Kobayashi, M. Kinugasa, Y. Nagamatsu, T. Majima, H. Ogita, J. Miyoshi, K. Hirata, Y. Takai, Role of afadin in vascular endothelial growth factor- and sphingosine 1-phosphate-induced angiogenesis, Circ Res 106 (2010) 1731-1742.

[20] A. Armulik, G. Genove, M. Mae, M.H. Nisancioglu, E. Wallgard, C. Niaudet, L. He, J. Norlin, P. Lindblom, K. Strittmatter, B.R. Johansson, C. Betsholtz, Pericytes regulate the blood-brain barrier, Nature 468 (2010) 557-561.

[21] G.A. Gundersen, G.F. Vindedal, O. Skare, E.A. Nagelhus, Evidence that pericytes regulate aquaporin-4 polarization in mouse cortical astrocytes, Brain Struct Funct 219 (2014) 2181-2186.

[22] R. Haddad-Tovolli, N.R.V. Dragano, A.F.S. Ramalho, L.A. Velloso, Development and Function of the Blood-Brain Barrier in the Context of Metabolic Control, Front Neurosci 11 (2017) 224.

[23] D. Bonkowski, V. Katyshev, R.D. Balabanov, A. Borisov, P. Dore-Duffy, The CNS microvascular pericyte: pericyte-astrocyte crosstalk in the regulation of tissue survival, Fluids Barriers CNS 8 (2011) 8.

[24] M.J. Menezes, F.K. McClenahan, C.V. Leiton, A. Aranmolate, X. Shan, H. Colognato, The extracellular matrix protein laminin alpha2 regulates the maturation and function of the blood-brain barrier, J Neurosci 34 (2014) 15260-15280.

[25] S. Noell, P. Fallier-Becker, U. Deutsch, A.F. Mack, H. Wolburg, Agrin defines polarized distribution of orthogonal arrays of particles in astrocytes, Cell Tissue Res 337 (2009) 185-195.

[26] M. Durbeej, Laminins, Cell Tissue Res 339 (2010) 259-268.

[27] M. Sixt, B. Engelhardt, F. Pausch, R. Hallmann, O. Wendler, L.M. Sorokin, Endothelial cell laminin isoforms, laminins 8 and 10, play decisive roles in T cell recruitment across the blood-brain barrier

in experimental autoimmune encephalomyelitis, J Cell Biol 153 (2001) 933-946.

[28] G. Gnanaguru, G. Bachay, S. Biswas, G. Pinzon-Duarte, D.D. Hunter, W.J. Brunken, Laminins containing the beta2 and gamma3 chains regulate astrocyte migration and angiogenesis in the retina, Development 140 (2013) 2050-2060.

[29] A.V. Molofsky, B. Deneen, Astrocyte development: A Guide for the Perplexed, Glia 63 (2015) 1320-1329.

Figures

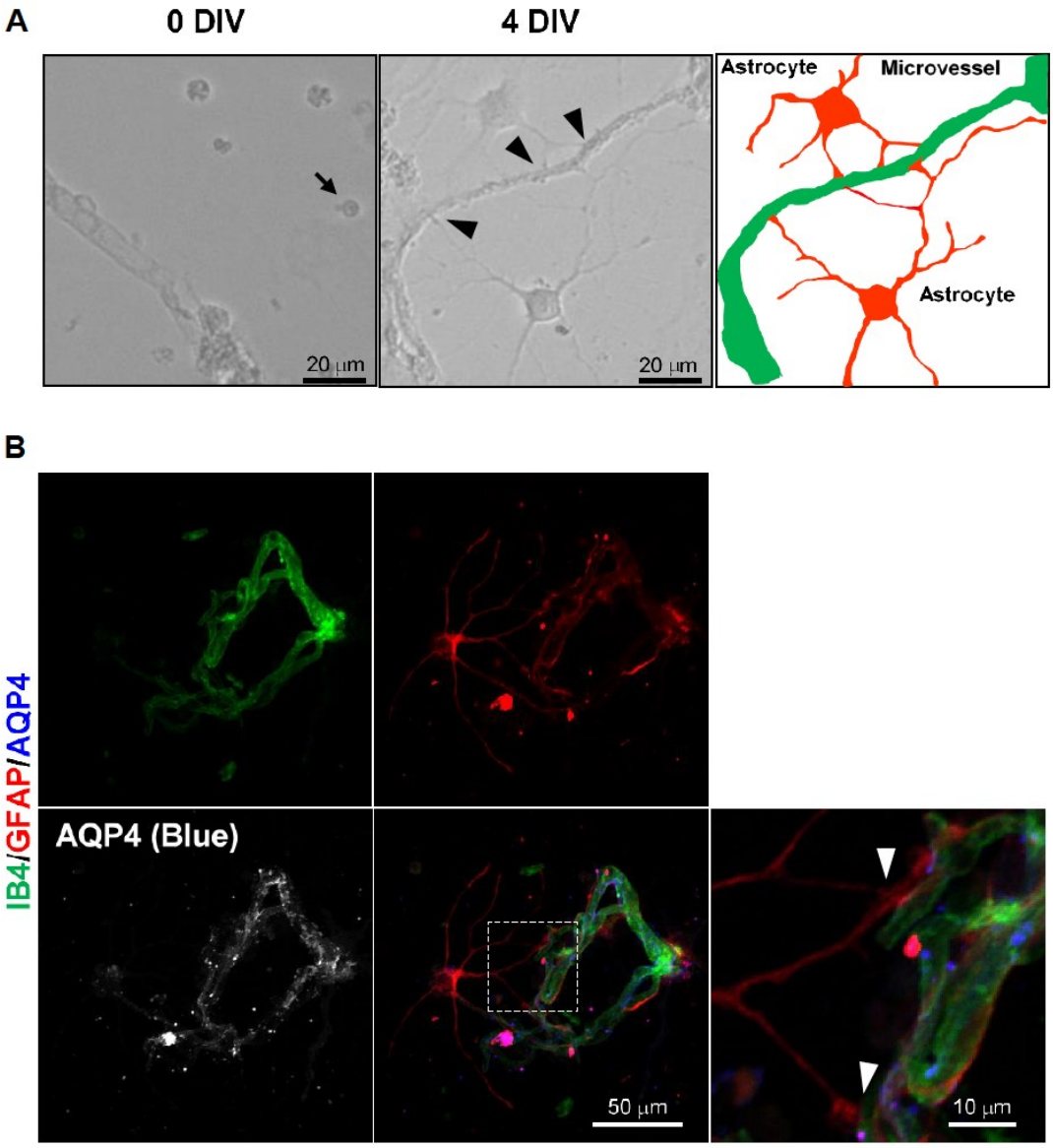

Figure 1. Contact formation between astrocytic processes and cerebral microvessels isolated from adult mice. A. Representative optical microscopic images at 0 and 4 DIV (*n* = 3). *Arrow*, astrocyte; *arrowheads*, contact sites. Illustration of the image at 4 DIV is shown on the right. **B**. Representative immunofluorescence images at 4 DIV (*n* = 3). Astrocytes and cerebral microvessels isolated from adult (13-week-old) mice were co-cultured for 4 DIV and stained with isolectin B4 (*IB4*, green) and antibodies to GFAP (red) and AQP4 (blue). A high-magnification image of the boxed area is shown on the right. *Arrowheads*, contact sites.

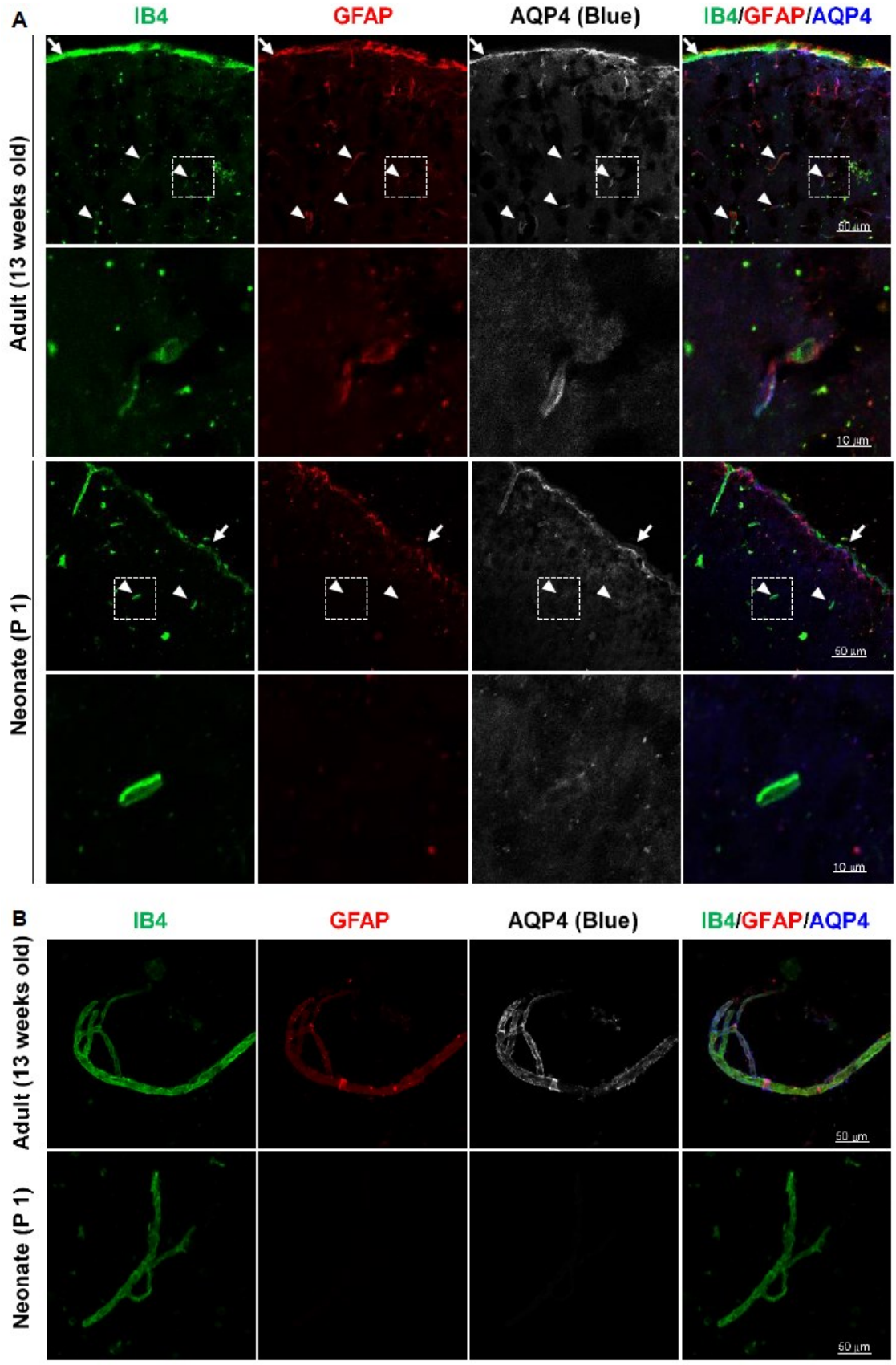
A
IB4
GFAP
AQP4 (Blue)
IB4/GFAP/AQP4
Adult (13 weeks old)
Neonate (P 1)
50 μm
10 μm
B
IB4
GFAP
AQP4 (Blue)
IB4/GFAP/AQP4
Adult (13 weeks old)
Neonate (P 1)
50 μm

Figure 2. Absence of GFAP and AQP4 expression around cerebral microvessels of neonatal mice. A. Cerebral sections. Cerebral sections prepared from adult (13-week-old) and neonatal (P1) mice were stained with isolectin B4 (*IB4*, green) and antibodies to GFAP (red) and AQP4 (blue). Representative immunofluorescence images are shown (n = 3). High-magnification images of the boxed area are shown in the lower panels. *Arrowheads*, colocalization at the cerebral parenchyma; *arrows*, colocalization at the cerebral surface. **B**. Cerebral microvessels isolated from adult (13-week-old) and neonatal (P1) mice were stained with isolectin B4 (*IB4*, green) and antibodies to GFAP (red) and AQP4 (blue). Representative immunofluorescence images are shown (n = 3).

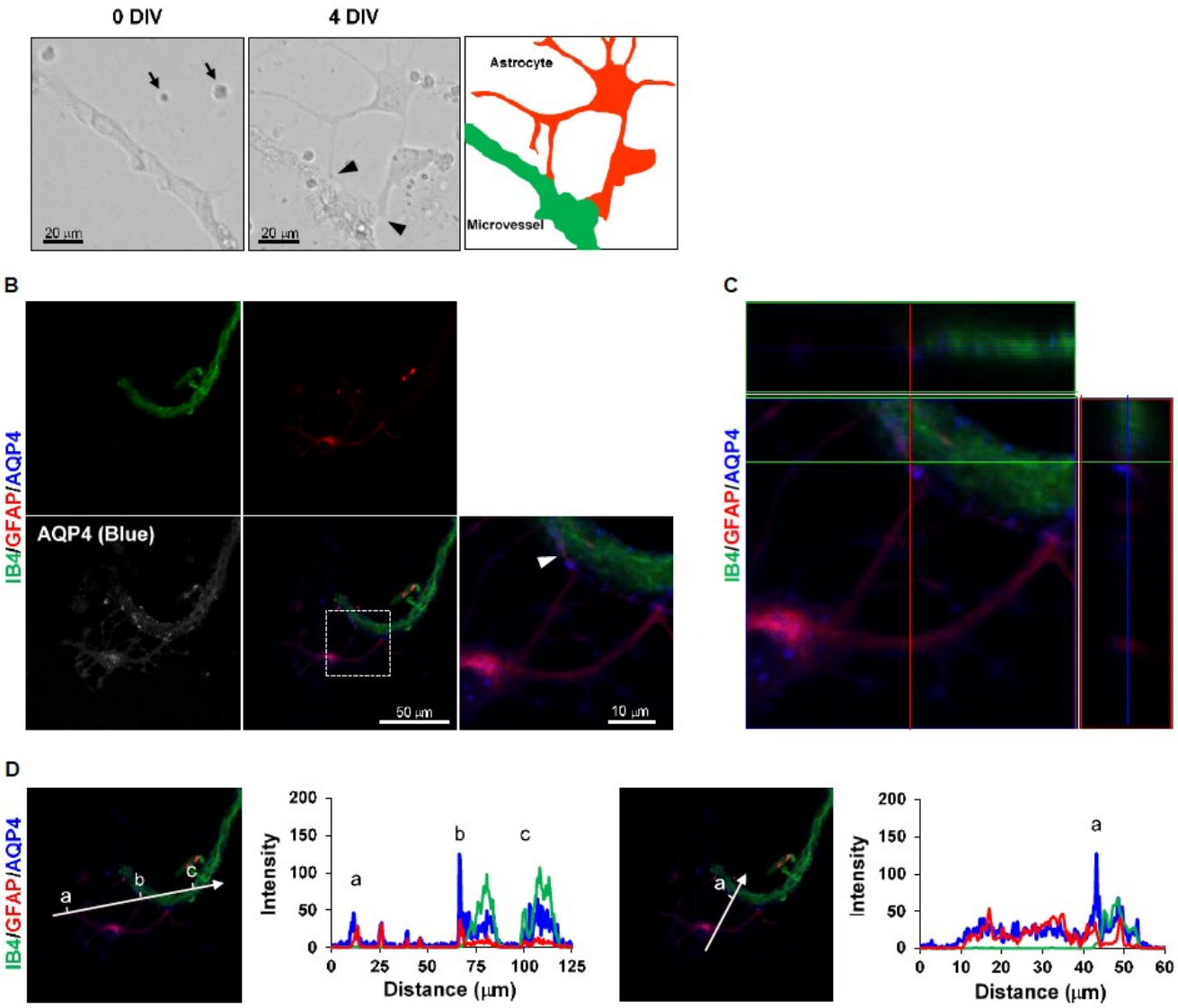

Figure 3. Contact formation between astrocytic processes and cerebral microvessels isolated from neonatal (P1) mice. A. Representative optical microscopy images at 0 and 4 DIV (*n* = 3). *Arrows*, astrocytes; *arrowheads*, contact sites. Illustration of the image at 4 DIV is shown on the right. **B**. Representative immunofluorescence images at 4 DIV. Astrocytes and cerebral microvessels isolated from neonatal (P1) mice were co-cultured for 4 DIV and stained with isolectin B4 (*IB4*, green) and antibodies to GFAP (red) and AQP4 (blue) (*n* = 3). A high-magnification image of the boxed area is shown on the right. *Arrowhead*, contact site. **C**. Orthogonal projection of Z-stacks through contact sites formed between astrocytic processes and cerebral microvessels isolated from neonatal mice, which were stained with isolectin B4 (*IB4*, green) and antibodies to GFAP (red) and AQP4 (blue). **D**: Intensity profiles of immunofluorescence signals for isolectin B4, GFAP, and AQP4.

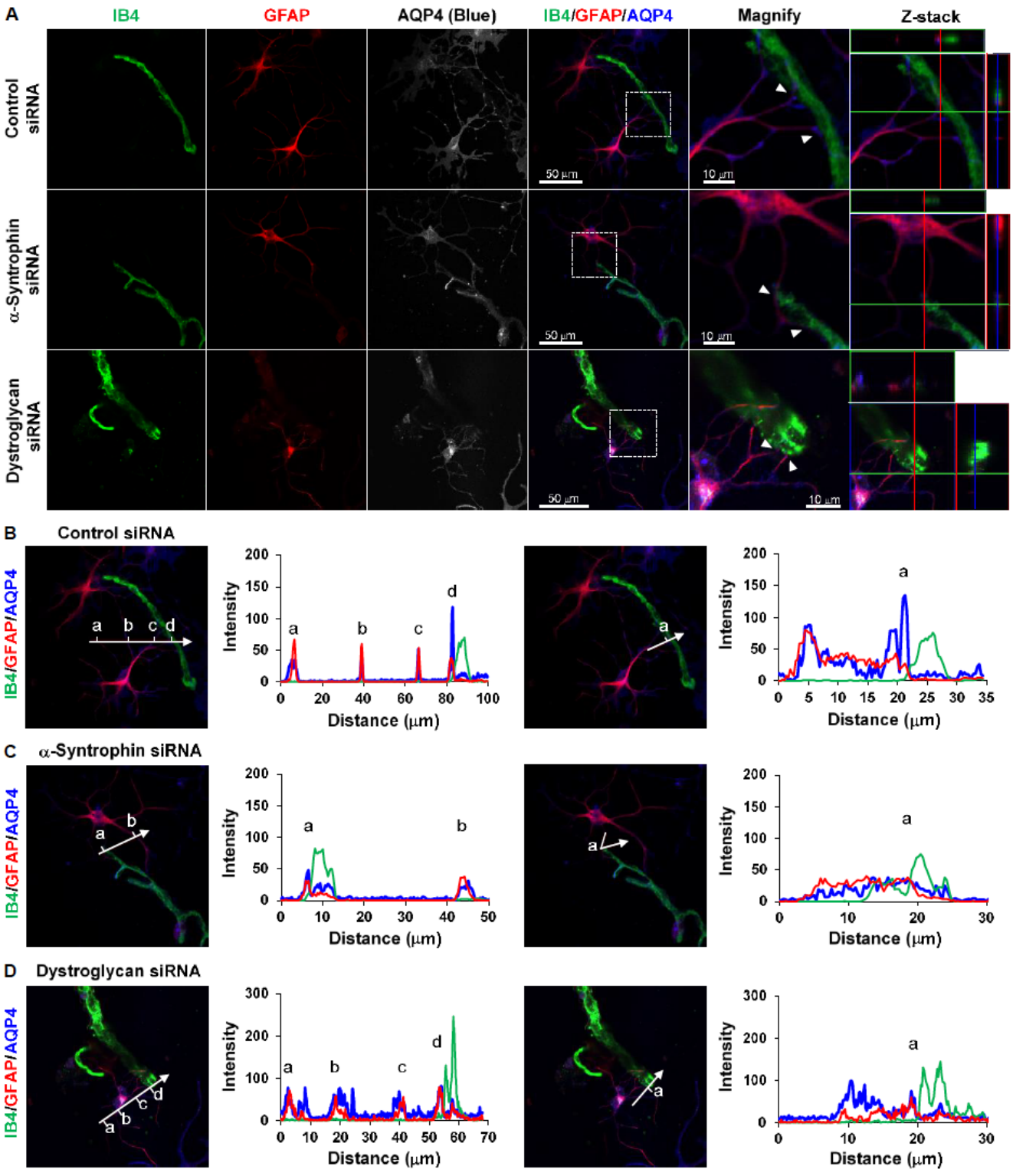

Figure 4. Effect of α-syntrophin and DG knockdown on concentration of immunofluorescence signal for AQP4 at contact sites between astrocytic processes and cerebral microvessels

isolated from neonatal mice. A. Effect of α-syntrophin and DG knockdown on contact formation between astrocytic processes and cerebral microvessels isolated from neonatal mice. Representative immunofluorescence image at 3 DIV are shown (*n* = 3). Magnified images represent high-magnification images of the boxed area. *Arrowheads*, contact sites. Orthogonal projection of Z-stacks through contact sites between astrocytic processes and cerebral microvessels isolated from neonatal mice are shown on the right. Cultures were stained with isolectin B4 (*IB4*, green) and antibodies to GFAP (red) and AQP4 (blue). **B–D**. Intensity profiles of AQP4 immunofluorescence staining in contact sites between astrocytic processes and cerebral microvessels isolated from neonatal mice.

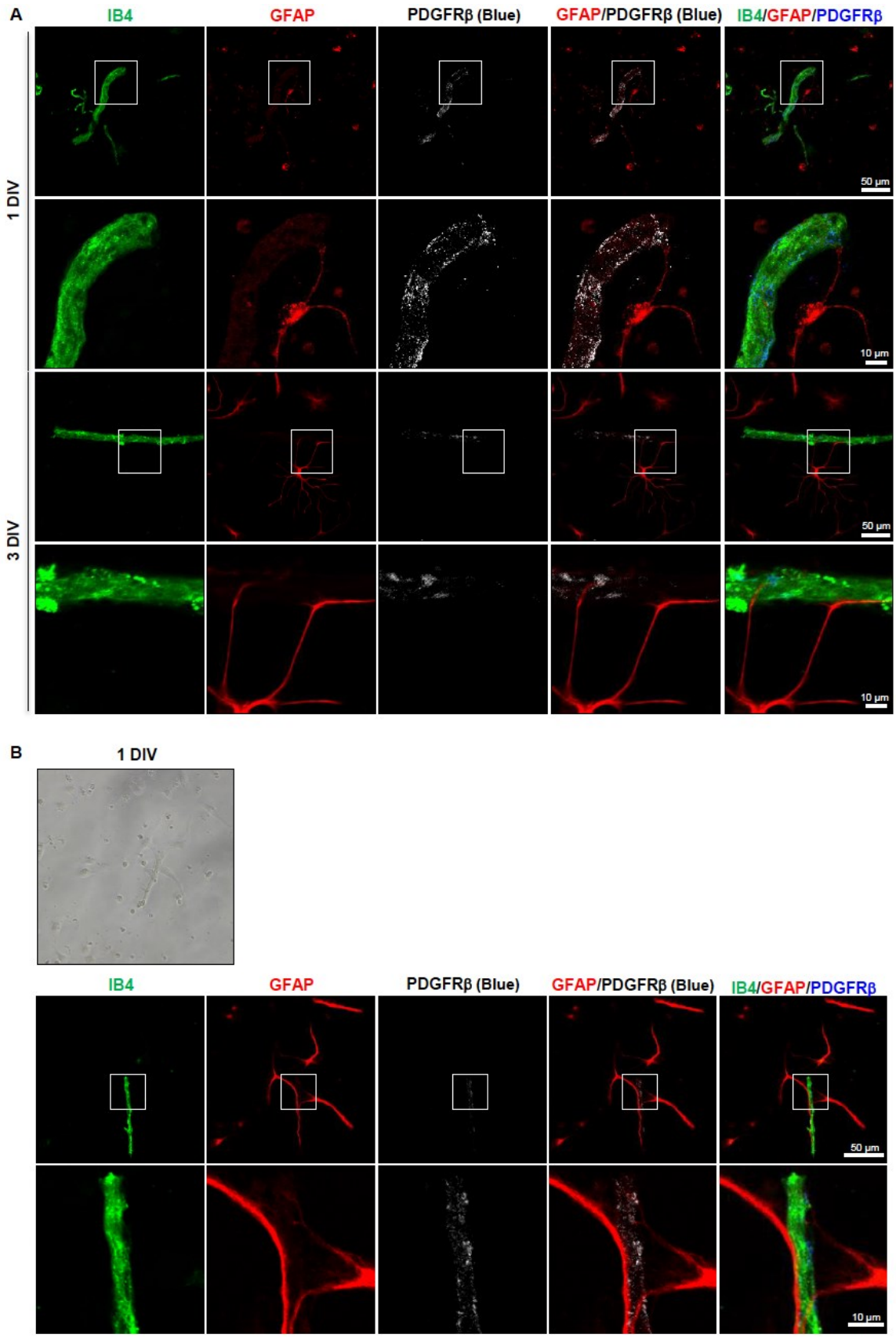
A
IB4
GFAP
PDGFRβ (Blue)
GFAP/PDGFRβ (Blue)
IB4/GFAP/PDGFRβ
1 DIV
3 DIV
50 μm
10 μm
50 μm
10 μm
B
1 DIV
IB4
GFAP
PDGFRβ (Blue)
GFAP/PDGFRβ (Blue)
IB4/GFAP/PDGFRβ
50 μm
10 μm

Figure 5. Predominant contact formation of astrocytic processes to pericytes is located at the abluminal surface of microvessels. A. Astrocytes and cerebral microvessels isolated from neonatal mice were co-cultured for 1 or 3 DIV and stained with isolectin B4 (*IB4*, green) and antibodies to GFAP (red) and PDGFRβ (blue). A representative immunofluorescence image is shown (*n* = 3). **B**. A snapshot of time-lapse images showing contact formation between an astrocytic process and a neonatal mouse microvessel (shown at the top). After time-lapse images were obtained, the sample was stained with isolectin B4 (*IB4*, green) and antibodies to GFAP (red) and PDGFRβ (blue). High-magnification images of the boxed area are shown in the lower panels.

Table 1. Frequency of contacts between astrocytes and PDGFRβ-positive areas in blood vessels

	1 DIV			3 DIV		
No. of contacts between a single astrocyte and a blood vessel	1	>2	Total	1	>2	Total
No. of contacts to PDGFRβ-positive region (A)	23	22	45	19	18	37
No. of contacts to PDGFRβ-negative region (B)	14	9	23	10	9	19
Proportion of (A) in (A)+(B) (%)	62.2	71.0	66.2	65.5	66.7	66.1
Ratio of (A) to (B)	1.6	2.4	2.0	1.9	2.0	1.9

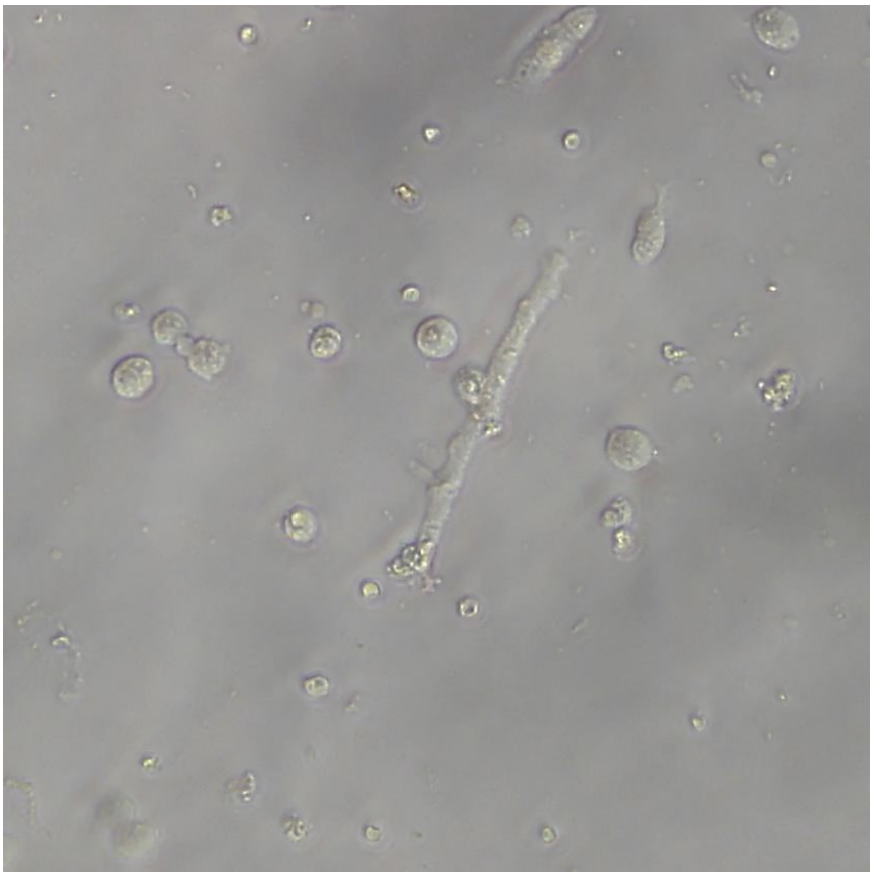

Movie 1. Time-lapse images of contact formation between an astrocytic process and a neonatal mouse microvessel.